

Growth mechanisms for InAs/GaAs QDs with and without Bi surfactants

X Y Chen¹, Y Gu^{*,1}, Y J Ma¹, S M Chen², M C Tang², Y Y Zhang², X Z Yu², P Wang¹, J Zhang¹, J Wu², H Y Liu², Y G Zhang¹

¹State Key Laboratory of Functional Materials for Informatics, Shanghai Institute of Microsystem and Information Technology, Chinese Academy of Sciences, Shanghai 200050, China

²Department of Electronic and Electrical Engineering, University College London, London WC1E 7JE, UK

Abstract: We report systematic study of growth of self-assembled InAs quantum dots (QDs) on GaAs substrate at various temperatures with and without exposure of bismuth surfactants. Results show that the coalescence amongst InAs QDs is considerably inhibited by the exposure of bismuth flux during growth in the temperature range from 475 to 500 °C, leading to improved dot uniformity and a modified dot density. The mechanism of the suppression effect by bismuth surfactants on the strain-induced islanding through inhibiting the indium adatom mobility and the evaporation rate on the surface kinetically is thus clarified for the growth of InAs QDs. The photoluminescence peak wavelength for the InAs QDs with Bi exposure red shifted slightly due to the suppression [of](#) Bi atoms on the QD dissolution during the capping process at higher temperatures. Moreover, by investigating the temperature-dependent quenching processes with and without Bi exposure, it is observed that the the weak carrier confinement occurred in QDs with the presence of Bi caused broadness in the linewidths.

* Corresponding author. Tel.: +86-21-62511070; fax: +86-21-52419931.
Email address: ygu@mail.sim.ac.cn (Y. Gu).

Keywords: InAs quantum dots; Bismuth; Surfactant; Molecular beam epitaxy

1 **1. Introduction**

2 Owing to the small segregation coefficient and low solid solubility in host lattice
3 [1], bismuth (Bi) is considered as an ideal surfactant for the material growth and has
4 recently been widely studied in different systems such as III-V quantum dots (QDs)
5 [2], quantum wells (QWs) [3], heteroepitaxy of Ge on Si [4], and Co/Cu multilayers
6 [5], etc. Most of these researches are devoted to improve the perfection of structures
7 in aspects of ordering, interfaces, and surfaces. Self-assembled InAs QDs on GaAs
8 (001) are favorable for devices operating in the optical telecom wavelength bands as
9 the improved height/diameter aspect provides a deeper confinement of the charge
10 carriers as compared to other nanostructures [6–8]. Given that QD-based device
11 performances will be affected by the dot density and dimension, the QD size,
12 uniformity, and density should be well tuned to guarantee optimum performances of
13 QD-based devices. For example, an improvement in QD density and uniformity has
14 the potential to increase the differential gain and modulation bandwidth for QD lasers
15 as well as the interband and intersubband absorption strength for QD-based
16 photodetectors. While the preserve of the shape and the improvement of uniformity of
17 InAs QDs using Bi surfactants have been verified in previous works either by
18 molecular beam epitaxy (MBE) or metal organic chemical vapor deposition (MOCVD)
19 [9, 10], whether Bi decreases or increases the surface migration of indium (In)
20 adatoms during the growth is still unclear since the effect of Bi surfactants during
21 InAs QD growth has been interpreted inconsistently. Some researchers hold the point
22 that Bi, acts as a reactive surfactant, can kinetically limit the surface adatom mobility

23 and decrease the In adatom diffusion length and thus increase the QD density [9, 10].
24 Others argue an opposite effect of Bi on the QD density and dimension [11]. Since the
25 QD density of uncapped QDs is greatly affected by not only the In adatom diffusion
26 length but also by the evaporation rate of InAs nuclei on the surface. Both processes
27 can be influenced by presence of Bi atoms and depends strongly on temperature. That
28 would be the reason why the controversy exists.

29 Here, we reconcile these apparent contradictions by comparing InAs QDs grown
30 with and without Bi exposure over the temperature range from 475 to 500 °C. It is
31 observed that the Bi surfactant leads to a decrease in QD density for lower growth
32 temperatures (475 - 485 °C), but an increase for higher growth temperatures (492 -
33 500 °C). The variations of the dot density are ascribed to the suppressing effect of Bi
34 surfactants on the In adatom surface diffusion length during MBE growth regardless
35 of growth temperatures, as is expected for a reactive surfactant [12]. Moreover, using
36 Bi as a surfactant enables an improvement in QD uniformity, suggesting that the Bi
37 surfactant-mediated growth of QDs has the potential to improve the performance of
38 QD-based optoelectronic devices.

39 **2. Experiments**

40 All the InAs/GaAs QD samples were grown by gas-source MBE in a VG
41 Semicon V90H system on semi-insulating GaAs (001) substrates. The structures were
42 started with a 200 nm GaAs buffer layer grown at 580 °C after desorption of the
43 native oxide layer. Then the substrate temperature was ramped down for the growth of
44 the first layer of InAs QDs with a thickness of nominal 2.8 monolayers (MLs) and

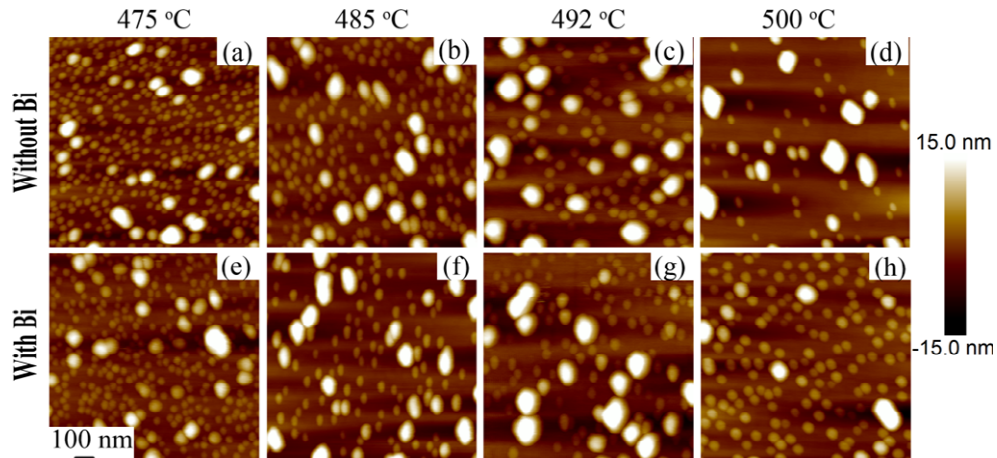
45 deposition rate of 0.07 ML/s. This QD layer was used for photoluminescence (PL)
46 measurements. A 10 nm GaAs capping layer was grown immediately at the same
47 temperature. Then the temperature was ramped up to 580 °C for the deposition of a
48 110 nm GaAs spacing layer. At last, the InAs QD layer was repeated on the surface of
49 the GaAs spacer for dot morphology studies. To investigate the effect of Bi exposure
50 on the InAs QDs, the Bi shutter was only opened during the deposition of QDs with
51 the Bi flux of 1.09 nA (Beam equivalent pressure $\sim 8.8 \times 10^{-9}$ torr), which has been
52 proved to be helpful for the growth of triangular highly strained InAs/InGaAs QWs
53 on InP [3], otherwise the Bi shutter remained closed during the growth. The substrate
54 temperatures of 475, 485, 492 and 500 °C were adopted for the deposition of InAs
55 QD layers. At such relatively high growth temperatures, Bi atoms tended to segregate,
56 floated on the growth surface without incorporating into the host material [13], and
57 acted evidently as a reactive surfactant. For comparison, another set of InAs QD
58 samples without Bi exposure was also grown on GaAs under nominally identical
59 growth conditions. Note that no deliberate growth interruption was used for both sets
60 of samples after the deposition of InAs QDs in an attempt to maintain the similarity
61 between the buried QDs and the uncapped QDs to the utmost, as well as to avoid
62 artificial impacts on the surface adatom (especially In) diffusion length. In this way,
63 the contrast between the two sets of QDs with and without Bi exposure would also be
64 enhanced. The nominal growth rate of GaAs was 0.16 nm/s. The V/III ratio was far
65 higher than 20 in this experiment according to our previous calibration, and As₂
66 species were used for all layers.

67 The InAs QD morphology was measured by a Bruker Icon atomic force
68 microscope (AFM) in the contact mode. The scanned area was $1 \times 1 \mu\text{m}^2$. PL spectra
69 were measured with a Nicolet IS50 Fourier transform infrared spectrometer (FTIR).
70 Samples were excited by a diode-pumped solid state (DPSS) laser ($\lambda = 532 \text{ nm}$).
71 Temperature-dependent PL measurements were carried out by mounting samples into
72 a continuous-flow helium cryostat, and a Lake Shore 330 temperature controller was
73 used to adjust the temperature from 10 to 300 K. The laser spot area was about $4.5 \times$
74 10^{-2} cm^2 . The laser power used in RT and temperature-dependent PL measurements
75 were about 340 and 136 mW, respectively.

76

77 3. Results and Discussion

78



79

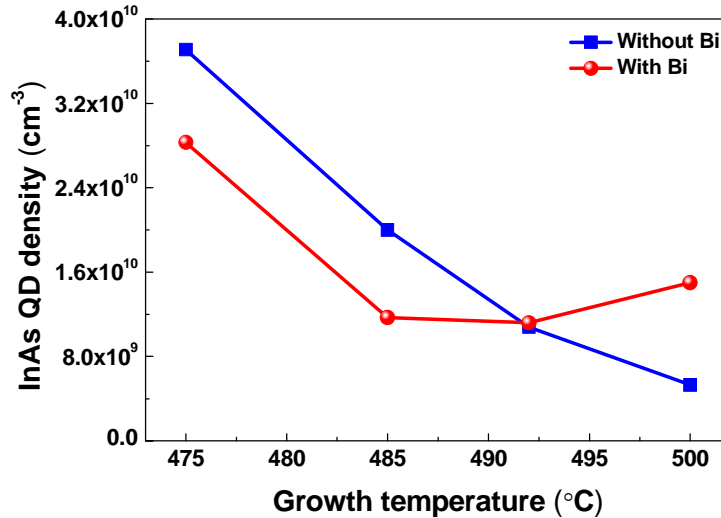
80 **Figure 1.** AFM images of InAs QDs grown at different temperatures with and without
81 Bi exposure.

82

83 Topographical AFM images of the grown InAs QDs without and with Bi
84 exposure are shown in figure 1. For the case of Bi-unmediated samples, at low
85 substrate temperatures, the surface population of free In adatoms diffused relatively

86 slowly due to a low surface energy and the average diffusion distance was short
87 before they combined with dissociated As₂ molecules. This results in a high dot
88 density with a small lateral size in general. At an elevated temperature, their diffusion
89 distances elongated, and dots coalesced with each other intensely with an increase in
90 surface energy of In adatoms, thus the dot density declined. As a concomitance of the
91 dot growing up, the random aggregation of islands increased, corresponding to the
92 piling up of bright circular features in figures 1(b) and 1(c). At the highest substrate
93 temperature of 500 °C, it was observed that big dots evolved into larger islands
94 leaving a few scattered dots surrounded, mostly caused by desorption of uncapped
95 QDs [and Ostwald ripening](#), as shown in figure 1(d). However, dissimilarities occurred
96 in both the dot density and dimension for the case of Bi-mediated samples, as shown
97 in figures 1(e)-1(h). The main difference can be found in the variation of dot densities
98 in comparison to that without the Bi exposure ranging from 475 to 500 °C. The InAs
99 dots formed under Bi exposure not only showed reduced variations in the dot
100 densities but also became more homogeneous especially in the case of 500 °C, where
101 the dislocated islands significantly suppressed, opposite to those without Bi exposure.
102 These results indicate that the Bi surfactants significantly modified the growth
103 kinetics of QDs. Bi atoms can preserve the dot dimension and density during cooling
104 down, similarly to the property of Sb atoms [14, 15].

105



106

107 **Figure 2.** The temperature-dependent InAs/GaAs QD densities with and without Bi
 108 exposure.

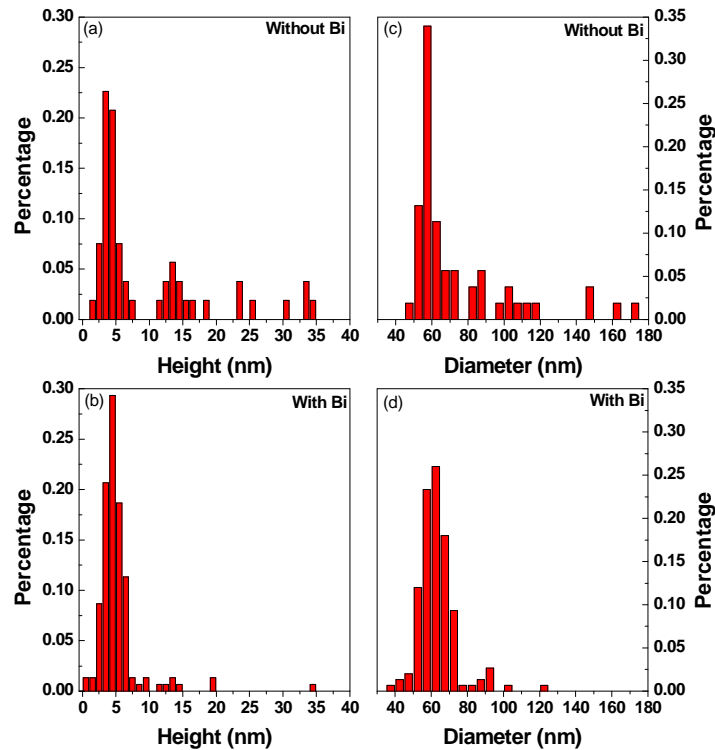
109

110 To quantify the influence of the Bi exposure on the QD densities,
 111 temperature-dependent InAs QD densities with and without Bi exposure were plotted
 112 in figure 2. Without Bi, the uncapped InAs QD densities decreased monotonically
 113 with the deposition temperature increasing from 475 to 500 °C mostly caused by the
 114 increase in desorption rates of In adatoms since they have additional time ~~to change~~
 115 ~~on~~ for surface changes during cooling down, especially for samples grown at higher
 116 temperatures. Nevertheless, the dot dimension and density of buried QDs can be quite
 117 different. It may be much higher in ~~both size and dot~~ density but smaller in size!
 118 However, when Bi exposure was used, the variation of the QD density differed
 119 considerably over the whole temperature range of 475 - 500 °C. It is obvious that the
 120 Bi-mediated QD ripening process during cooling down is suppressed by Bi atoms. As
 121 a result, QDs with Bi exposure showed a decrease in the overall density at low

122 temperatures but an increase at high temperatures compared to the QDs without Bi
123 exposure.

124 It is well known that the InAs dot density and dimension depend strongly upon
125 factors such as the surface diffusion length of In adatoms [16], the desorption rate of
126 In adatoms from the substrate surface and the dissociation rate for the tiny InAs nuclei
127 [17]. It is supposed that the dominant factors for QD density and dimension should be
128 varied over the variation range of temperatures, which will be strengthened by the
129 employment of Bi surfactants for the QD growth. At low temperatures, little
130 desorption of In adatoms and dissociation for the tiny InAs nuclei occur. The dot
131 density is probably dominated by the diffusion length of In adatoms on surface, and
132 the reduction of the surface diffusion length of In adatoms due to the presence of Bi
133 undoubtedly will defer the InAs QD formation by delaying the onset of QDs, leading
134 to a decrease in the overall QD density with respect to the case without Bi exposure.
135 At high temperatures, the desorption of In adatoms from the growth surface and the
136 dissociation for the tiny InAs nuclei aggravate intensely, but they are ultimately
137 suppressed by the presence of Bi. While the suppression effect of Bi exposure on the
138 dot coalescence still exists due to the restrained surface diffusion length of In adatoms,
139 thus leading to a higher QD density instead compared to that without Bi exposure.

140 These results demonstrate the suppression effect of Bi surfactants on the In
141 adatom surface diffusion, which eventually leads to a suppression of QD coalescence
142 and ripening, similar to the behavior of antimony (Sb) surfactants for QD growth [18,
143 19].



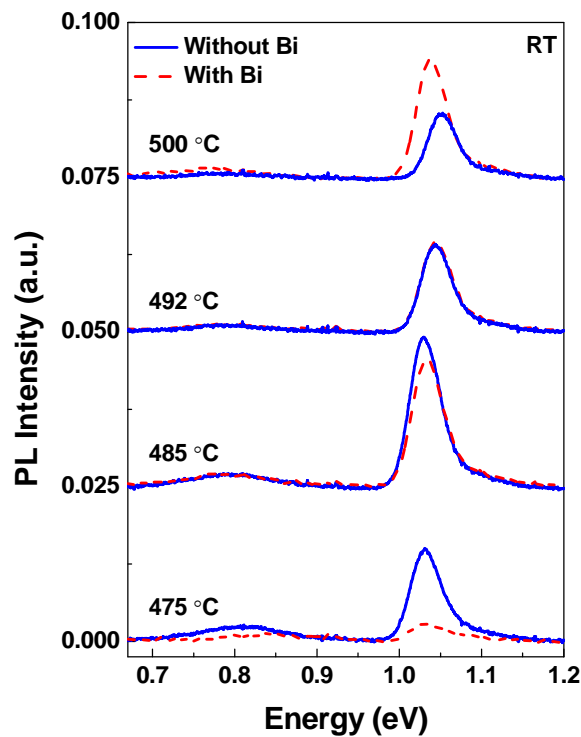
145

146 **Figure 3.** The histograms of the InAs QD height and diameter distribution grown at
 147 500 °C with and without Bi exposure.

148

149 To analyze the effects of the Bi surfactant on QD uniformity, the typical height
 150 and diameter histograms of the InAs QDs grown at 500 °C with and without Bi
 151 exposure were extracted from the AFM images, as shown in figure 3. From the
 152 histograms of height distribution, as shown in figures 3(a) and 3(b), an extremely
 153 large proportion of QDs with the height beyond 12 nm was suppressed markedly after
 154 the Bi exposure. The dot height in the presence of Bi showed less size fluctuation than
 155 that without Bi. The average heights were deduced to be 6.3 and 10.5 nm for InAs
 156 QDs with and without Bi exposure, respectively. Similarly, QDs grown without Bi
 157 exhibited a wider distribution in the diameter, as shown in figure 3(c). While the
 158 fluctuation in the diameter was diminished for the InAs QDs in the presence of Bi,

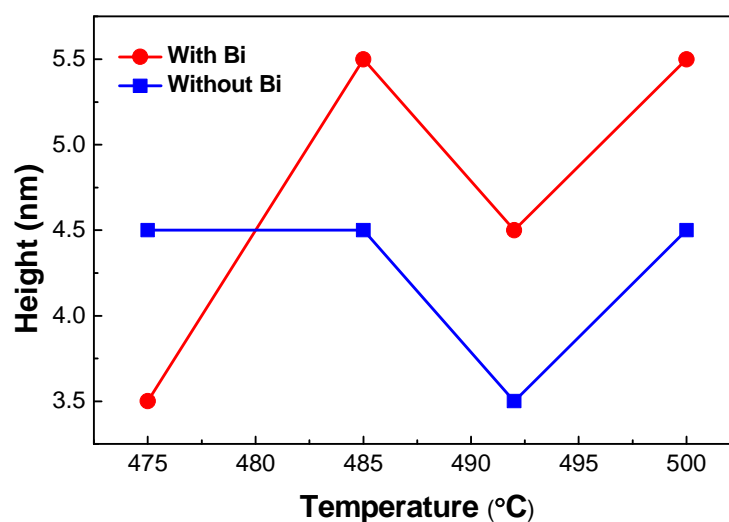
159 and the average QD diameters were deduced to be 64.0 and 74.2 nm for InAs QDs
160 with and without Bi exposure, respectively. This means that the Bi surfactant
161 decreased the typical QD size through suppressing the free surface diffusion of In
162 adatoms during InAs QD growth. This also coincides with the QDs grown with Sb as
163 a surfactant [18, 19].



164
165 **Figure 4.** PL spectra of InAs QDs grown at different temperatures with and without
166 Bi exposure.

167 Figure 4 shows the room temperature (RT) PL spectra for the InAs QDs with and
168 without Bi exposure deposited at different temperatures. The output voltage of the
169 DPSS laser was set to 2.5 V with an excitation power of about 340 mW. As shown in
170 figure 4, the ground state emission occurred at about 1.03 eV for both sets of QD
171 structures at RT. The broad signal located in the 0.75-0.87 eV range fell off linearly as
172 the temperature increased, corresponding well with the features of the lateral

173 associated InAs QDs [20, 21]. It is noticeable that the peak position of the ground
174 state emission for the InAs QDs with Bi exposure shifted slightly to the red,
175 especially for the InAs QDs and the GaAs capping layer grown at higher temperatures
176 (500 °C) with respect to those without Bi exposure as shown in figure 3. This
177 phenomenon can be explained by the fact that QDs will be partly dissolved ~~with a~~
178 ~~lower height~~ during the capping process [22, 23], and as a result their height is lower,
179 but the presence of Bi atoms can definitely influence this process by suppression of
180 QD dissolution and then increase the height of resulting QDs, which is similar to Sb
181 atoms [14, 15]. As a result, this shifts the wavelength of InAs QDs grown with Bi to
182 lower energies. It is worth noting that the bigger hillocks may not show any PL since
183 they are relaxed and contain ~~annihilation centers~~ dislocations. The PL spectrum
184 originated only from the small QDs with the height not bigger than 10 nm - the first
185 maximum in the histogram for both samples shown in figures 3 (a) and (b). This
186 redshift of PL agrees well with the first maximum shifted to bigger QD size for
187 sample grown with Bi at higher temperatures, as shown in figure 5.



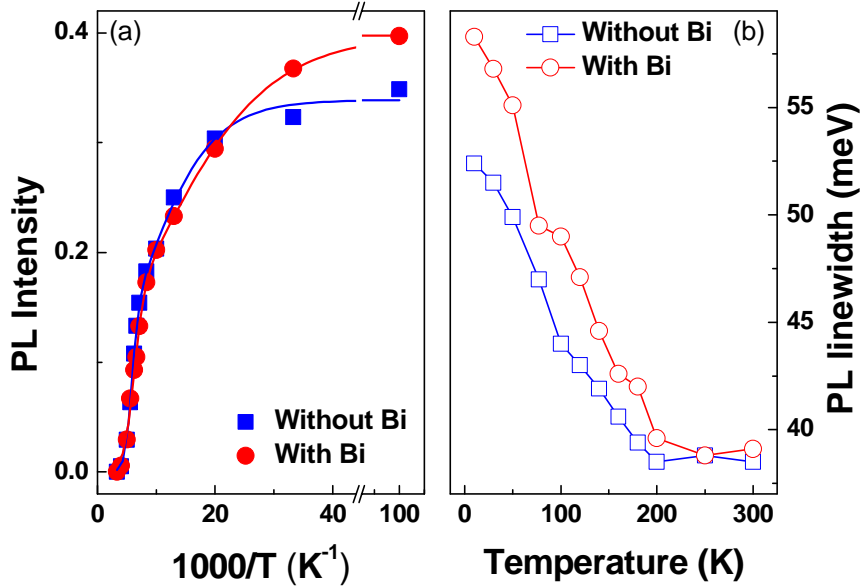
188

189 Figure 5. The peak height value for smaller QDs and its dependence on the

190 [temperature.](#)

191 Additionally, the PL intensity of the ground state transition for InAs/GaAs QDs
192 with Bi exposure was weaker at a deposition temperature of 475 °C but comparable at
193 temperatures of 485 - 500 °C with respect to those without Bi exposure. Since Bi
194 induced layer-by-layer growth in the InAs/GaAs strained systems by reducing the
195 interface energy, and thus the three-dimensional (3D) islands in the
196 Stranski-Krastanov (S-K) growth mode was suppressed. This would lead to
197 postponement of the wetting layer formation before the growth mode changing from
198 2D to 3D during the S-K growth process due to the decrease in the strain energy [9,
199 24]. Then the critical thickness of the wetting layer would be extended, which delayed
200 the formation of InAs QDs. If this wetting layer was modified properly, it would
201 improve the optical property of InAs QDs, but a much thicker one, in turn, could
202 damage it by serving as a channel for thermally activated carriers [25]. The influence
203 could change with the growth temperature due to the variation of the critical thickness
204 of the wetting layer. The inferior PL of InAs QDs grown with Bi exposure at 475 °C
205 could be caused by the insufficiently developed QDs at this low temperature with the
206 presence of Bi atoms.

207



208

209 **Figure 5.6.** (a) Integrated PL intensities for InAs QDs grown at 492 °C with and
 210 without Bi exposure as a function of reciprocal temperature from 10 K to 300 K. The
 211 lines are the least squares fit of the data. (b) PL linewidths for InAs QDs with and
 212 without Bi exposure versus temperatures. The lines are drawn as a guide.

213

214 To have a deeper understanding of the effect of Bi surfactants on the optical
 215 properties of QDs, the change of carrier confinement in both sets of QDs should be
 216 investigated further by measuring temperature-dependent PL quenching processes.
 217 Therefore, the InAs QDs grown at 492 °C with similar RT PL spectra under both
 218 Bi-mediated and unmediated conditions to eliminate the impact coming from different
 219 dot densities were measured. The integrated PL intensities, excited under low-pump
 220 conditions, were plotted in figure 5.6(a) as a function of reciprocal temperature. The
 221 fits are derived by applying equation [26], $I(T) = I(0)/[1 + C_1 \exp(-E_1/k_B T) +$
 222 $C_2 \exp(-E_2/k_B T)]$ (Eq. (1)), where C_1 and C_2 represent the strengths of the both
 223 quenching processes, $I(T)$ and $I(0)$ are the PL integrated intensity at temperature T and
 224 0 K, k_B is Boltzmann' constant and E_1 , E_2 are the thermal activation energies

225 corresponding to the highest required energies for carriers to escape from the active
226 region in low- and high- temperature regions respectively. Experimental data were
227 well fitted as shown in figure 5_6(a), and the fitting parameters calculated from the
228 Arrhenius plots were listed in table 1.

229 It can be observed that calculated activation energies were 14.6 and 9.0 meV in
230 low-temperature regions, 156.1 and 105.0 meV in high-temperature regions for the
231 InAs QDs without and with Bi exposure respectively. The reduction in activation
232 energies of E_1 and E_2 suggested weaker carrier confinement for InAs QDs with Bi
233 exposure. This reduced confinement potential can be explained by the fact that the
234 size of QDs at lower temperatures with Bi as surfactant is smaller, which decreases
235 the confinement barrier for carriers in QDs [11].

236 Lastly, the PL linewidths for InAs QDs grown at 492 °C with and without Bi
237 exposure as a function of temperature from 10 to 300 K were plotted in figure 5_6(b).
238 The linewidths of both spectra substantially increased in low-temperature regions due
239 to the appearance of emission from small QDs [27]. While at high temperatures, the
240 QDs with high localization energies will be preferentially occupied by carriers and
241 thus dominated the spectra, resulting in narrow linewidths. It is noted that the
242 linewidths were broadened lightly for QDs with Bi exposure over the temperature
243 range of 10-300 K, which also indicates that a weak carrier confinement occurred in
244 the QDs grown with the presence of Bi.

245

246 **Table 1.** Fitting parameters for the measured temperature-dependent integrated PL
247 intensities of InAs QDs with and without Bi.

248

Table 1.

Sample	$I(0)$	E_1	C_1	E_2	C_2
Without Bi	0.34	14.6	3.4	156.1	73943
With Bi	0.40	9.0	2.7	105.0	3951.9

249

250 **4. Conclusions**

251 The influence of Bi exposure on the self-assembled InAs/GaAs QDs has been
 252 investigated by comparison of dot density and dimension at varying substrate
 253 temperatures. It is shown that the dot density decreases but large, defective InAs
 254 islands accumulate as the growth temperature increases under the Bi-unmediated
 255 condition. By contrast, for the Bi-mediated growth, the dot areal density decreases at
 256 low temperatures but increases at high temperatures, which reveals essentially the
 257 suppression effect of Bi on the surface migration and desorption of In adatoms.
 258 Furthermore, the QD dimensions become more uniform and homogeneous at higher
 259 temperatures for Bi atoms suppressing the formation of larger dislocated islands. If
 260 the negative effect of Bi can be avoided, Bi-mediated QDs could show great
 261 application potential for photonic and optoelectronic devices in the future.

262

263 **Acknowledgments**

264 The authors wish to acknowledge the support of the National Key Research and
 265 Development Program of China under Grant No. 2016YFB0402400, the National
 266 Natural Science Foundation of China under grant Nos. 61675225, 61605232 and
 267 61775228.

268 **References**

- 269 [1] Sakamoto K, Kyoya K, Miki K, Matsuhata H and Sakamoto T 1993 Which
270 Surfactant Shall We Choose for the Heteroepitaxy of Ge/Si(001)? -Bi as a Surfactant
271 with Small Self-Incorporation- *Jpn. J. Appl. Phys.* **32** L204–L206.
- 272 [2] Okamoto H, Tawara T, Gotoh H, Kamada H and Sogawa T 2010 Growth and
273 Characterization of Telecommunication-Wavelength Quantum Dots Using Bi as a
274 Surfactant *Jpn. J. Appl. Phys.* **49** 06GJ01.
- 275 [3] Gu Y, Zhang Y G, Chen X Y, Xi S P, Du B and Ma Y J 2015 Effect of bismuth
276 surfactant on InP-based highly strained InAs/InGaAs triangular quantum wells *Appl.*
277 *Phys. Lett.* **107** 212104.
- 278 [4] Paul N, Asaoka H, Myslivecek J and Voigtlander B 2004 Growth mechanisms in
279 Ge/Si(111) heteroepitaxy with and without Bi as a surfactant *Phys. Rev. B* **69**
280 193402.
- 281 [5] Polit A, Kac M, Krupinski M, Samul B, Zabala Y and Marszalek M 2007 The
282 Behaviour of Surfactants during the Growth of Co/Cu Multilayers *Acta Phys. Pol. A*
283 **112** 1281–1287.
- 284 [6] Yang Y, Jo B, Kim J, Lee C R, Kim J S, Oh D K, Kim J S and Leem J Y 2009
285 Optical stability of shape-engineered InAs/InAlGaAs quantum dots *J. Appl. Phys.* **105**
286 053510.
- 287 [7] Saito H, Nishi K, Kamei A and Sugou S 2000 Low chirp observed in directly
288 modulated quantum dot lasers *IEEE Photon. Technol. Lett.* **12** 1298–1300.
- 289 [8] Chen S M *et al* 2016 Electrically pumped continuous-wave III-V quantum dot

290 lasers on silicon *Nat. Photonics* **10** 307–311.

291 [9] Dasika V D, Krivoy E M, Nair H P, Maddox S J, Park K W, Jung D, Lee M L, Yu
292 E T and Bank S R 2014 Increased InAs quantum dot size and density using bismuth
293 as a surfactant *Appl. Phys. Lett.* **105** 253104.

294 [10] Zvonkov B N, Karpovich I A, Baidus N V, Filatov D O, Morozov S V and
295 Gushina Y Y 2000 Surfactant effect of bismuth in the MOVPE growth of the InAs
296 quantum dots on GaAs *Nanotechnology* **11** 221–226.

297 [11] Fan D S, Zeng Z Q, Dorogan V G, Hirono Y, Li C, Mazur Y I, Yu S Q, Johnson
298 S R, Wang Z M, Salamo G J 2013 Bismuth surfactant mediated growth of InAs
299 quantum dots by molecular beam epitaxy *J Mater Sci: Mater Electron* **24** 1635–1639.

300 [12] Massies J and Grandjean N 1993 Surfactant effect on the surface diffusion length
301 in epitaxial growth *Phys. Rev. B* **48** 8502.

302 [13] Feng G, Oe K, Yoshimoto M 2007 Temperature dependence of Bi behavior in
303 MBE growth of InGaAs/InP *J. Cryst. Growth* **301–302** 121–124.

304 [14] Matsuura T, Miyamoto T, and Koyama F 2006 Topological characteristics of
305 InAs quantum dot with GaInAs cover using Sb surfactant *Appl. Phys. Lett.* **88**
306 183109.

307 [15] Guimard D, Nishioka M, Tsukamoto S, Arakawa Y 2007 Effect of antimony on
308 the density of InAs/Sb:GaAs(100) quantum dots grown by metalorganic
309 chemical-vapor deposition *J. Cryst. Growth* **298** 548–552.

310 [16] Chu L, Arzberger M, Böhm G and Abstreiter G 1999 Influence of growth
311 conditions on the photoluminescence of self-assembled InAs/GaAs quantum dots *J*

312 *Appl. Phys.* **85** 2355.

313 [17] Ajayan P M, Carlson J, Bayburt T and Nalwa H S (editor) 2002 Nanostructured
314 materials and nanotechnology (Academic Press).

315 [18] Kakuda N, Yoshida T and Yamaguchi K 2008 Sb-mediated growth of
316 high-density InAs quantum dots and GaAsSb embedding growth by MBE *Appl. Surf.*
317 *Sci.* **254** 8050–8053.

318 [19] Guimard D, Nishioka M, Tsukamoto S and Arakawa Y 2007 Effect of antimony
319 on the density of InAs/Sb:GaAs(100) quantum dots grown by metalorganic
320 chemical-vapor deposition *J. Cryst. Growth* **298** 548–552.

321 [20] Zhukov A E, Volovik B V, Mikhrin S S, Maleev N A, Tsatsul'nikov A F, Nikitina
322 E V, Kayander I N, Ustinov V M and Ledentsov N N 2001 1.55–1.6 μm
323 electroluminescence of GaAs based diode structures with quantum dots *Tech. Phys.*
324 *Lett.* **27** 734–736.

325 [21] Tonkikh A A, Cirlin G E, Talalaev V G, Novikov B V, Egorov V A, Polyakov N
326 K, Samsonenko Yu B, Ustinov V M, Zakharov N D, Werner P 2003
327 Room-temperature 1.5–1.6 μm photoluminescence from InGaAs/GaAs
328 heterostructures grown at low substrate temperature *Semiconductors* **37** 1406–1410.

329 [22] Hospodková A, Vyskočil J, Pangrác J, Oswald J, Hulicius E, Kuldová K 2010
330 Surface processes during growth of InAs/GaAs quantum dot structures monitored by
331 reflectance anisotropy spectroscopy *Surf. Sci.* **604** 318–321.

332 [23] Utrilla A D *et al* 2018 Size and shape tunability of self-assembled InAs/GaAs
333 nanostructures through the capping rate *Appl. Surf. Sci.* **444** 260–266.

- 334 [24] Matsuura T, Miyamoto T, Kageyama T, Ohta M, Matsui Y, Furuhata T and
335 Koyama F 2004 Surfactant Effect of Sb on GaInAs Quantum Dots Grown by
336 Molecular Beam Epitaxy *Jpn. J. Appl. Phys.* **43** L605–L607.
- 337 [25] Kudrawiec R and Misiewicz J 2009 Photoreflectance and contactless
338 electroreflectance measurements of semiconductor structures by using bright and dark
339 configurations 2009 *Rev. Sci. Instrum.* **80** 096103.
- 340 [26] Gu Y, Zhang Y G, Li A Z, Wang K, Li C and Li Y Y 2009 Structural and
341 Photoluminescence Properties for Highly Strain-Compensated InGaAs/InAlAs
342 Superlattice *Chin. Phys. Lett.* **26** 077808.
- 343 [27] Bouzaïene L, Saidi F, Sfaxi L and Maaref H 2010 Temperature dependence of the
344 optical properties of InAs quantum dots with bimodal size evolution grown on GaAs
345 (115)A substrate *Physica B* **405** 744–747.